JOURNAL OF GEOPHYSICAL RESEARCH, VOL. 106, NO. E8, PAGES 17,505-17,513, AUGUST 25, 2001

Ancient Martian volcanoes in the Aeolis region: New evidence from MOLA data

Emily M. Stewart and James W. Head

Department of Geological Sciences, Brown University, Providence, Rhode Island

Abstract. Mars Orbiter Laser Altimeter (MOLA) altimetric data confirm the volcanic origin of a Noachian-aged hilly feature (Zephyria Tholus) in the Aeolis area of Mars. Similar characteristics shared by at least one nearby topographic high suggest that volcanic activity represented by such features may have been more widespread than previously thought. Morphological structures and morphometric data for Zephyria are consistent with a stratovolcano origin, in which the edifice formed by mixed explosive and effusive eruptions, and was altered by subsequent flank erosion, to produce a distinctive truncated cone with concave upward flanks. Criteria are outlined to help detect and distinguish the origin of such features in other ancient regions of Mars.

1. Introduction

An unusually symmetrical cone located in the Aeolis region of Mars (20°S, 187°W) with a flat-floored summit crater and distinctive radial dissection of its flanks was first recognized by *Greeley and Spudis* [1978] and interpreted to have a volcanic origin (Feature A, Plate 1). In their global survey of Martian volcanoes, *Hodges and Moore* [1994] described the feature as a single, symmetric, cratered cone in the hilly Noachian highlands with a basal diameter of ~30 km and a circular summit crater 8 km across. On the basis of its shape and its striking morphological similarity to Earth stratovolcanoes (e.g. Tongariro in New Zealand; Figure 41B of *Hodges and Moore* [1994]), they interpreted this feature to be the best candidate in their global survey for a composite cone or stratovolcano. Tongariro volcano is a truncated composite cone composed of andesitic ash and lava flows which has subsequently undergone flank erosion by glaciers and streams [*Gregg*, 1960].

Feature A (Zephyria Tholus) is formed within the hilly unit of the lower Noachian highland plateau sequence (Nplh), one of the oldest recognized stratigraphic units on Mars [*Scott and Tanaka*, 1986]. Nplh consists of rough, hilly, and fractured material with locally high relief and is inferred to be ancient highland rocks and impact breccia produced during the period of heavy bombardment. In the Aeolis region, occurrences of Nplh are surrounded by highly cratered, fractured, and channelized material mapped as Npl_1, which is thought to consist of a mixture of volcanic materials, erosional products, and impact breccias of middle Noachian age [*Scott and Tanaka*, 1986; *Greeley and Guest*, 1987]. Feature A is thus interpreted to be a very ancient structure, remarkably pristine for its age (Plate 1). Zephyria Tholus is located at the head of Durius Valles, which consists of several flat-floored tributaries incised into the cratered highlands of Terra Cimmeria. These tributaries converge into a single channel before emptying into De Vaucolueurs, a ~300 km diameter degraded impact basin [*Nelson et al.*, 2001a]. Zephyria Tholus may be related to the source and origin of Durius Valles [*Nelson et al.*, 2001b].

Paper number 2000JE001322.
0148-0227/01/2000JE001322$09 00

As on Earth, the topographic and slope characteristics of Feature A could provide information about its eruptive history. In this paper we use Mars Orbiter Laser Altimeter (MOLA) topographic data [*Smith et al.*, 1998, 1999; *Zuber et al.*, 2000] to study the shapes and slope characteristics of this feature and to assess its origin. Furthermore, we examine the characteristics of other, more degraded topographic highs nearby to assess the likelihood that they represent the same class of feature, and thus have the same origin, as Feature A.

2. Stratovolcanoes on Earth

On Earth, composite volcanoes or stratovolcanoes are relatively large constructional volcanic features built of layers of small-volume lava flows and pyroclastic deposits [*Bates and Jackson*, 1984], unlike shield volcanoes, which are built predominantly of lava flows with a wider range of lengths. The greater explosiveness of stratovolcano eruptions relative to shield volcano effusions is usually attributed to higher viscosity and/or volatile content of stratovolcano magmas [*Cas and Wright*, 1987, pp. 386-390]. The pyroclastic deposits and lava flows associated with stratovolcanoes tend to accumulate in the near-vent area, contributing to smaller basal diameter (30-100 km) and steeper flank slopes (as high as 35°) than those typical of shield volcanoes [*Walker*, 2000; *Davidson and de Silva*, 2000]. Terrestrial arc stratovolcanoes are typically 2-2.5 km in height, while intraplate structures can be as tall as 3.7 km [*Walker*, 2000]. In profile, young stratovolcanoes have a simple conical shape. Older stratovolcanoes commonly have concave upward flank profiles as a result of fluvial dissection or sector collapse [e.g., *Reid et al.*, 2000]; truncation of the upper slopes by caldera formation (by explosion or collapse) also occurs. Stratovolcanoes are typically found in chains on the overriding plate of convergent plate margins, with intervolcano spacings comparable to their diameters (30-100 km). Exceptions include some edifices found on Iceland and some associated with the East African Rift.

3. Volcanism and Stratovolcanoes on Mars

Volcanic edifices on Mars include the giant central vent volcanoes (e.g. Olympus and Elysium Montes), paterae, tholi,

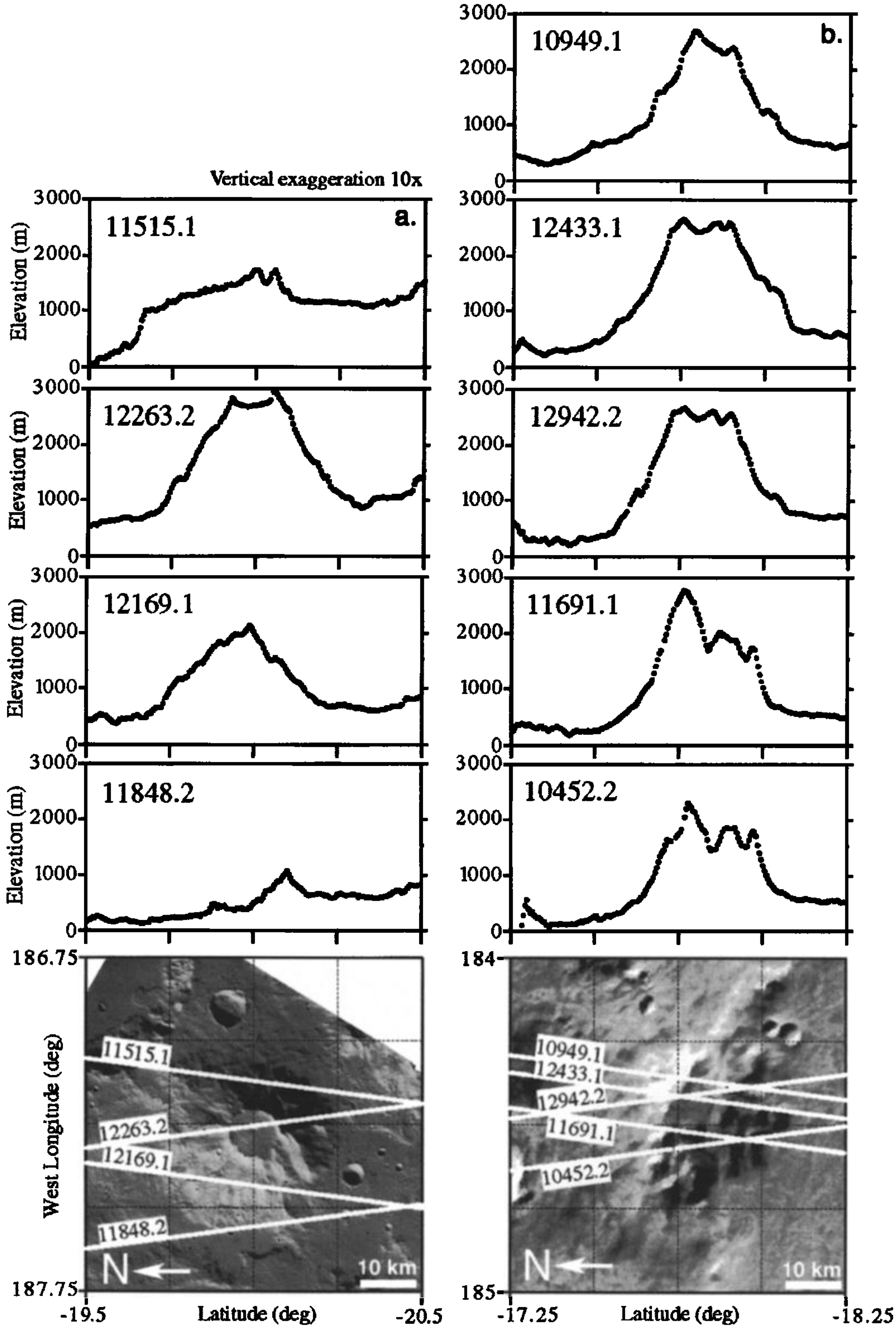

Figure 1. MOLA altimetry data for several candidate features: (a) MOLA profiles across Feature A and (b) MOLA profiles across Feature B. Here and in all other figures, zero reference is MOLA-derived mean radius (see *Smith et al.* [1998, 1999] and *Zuber et al.* [2000] for details). Points are individual MOLA data points, and numbers refer to profile number. North is to the left in both images.

cones, and small shields [*Hodges and Moore*, 1994; *Zimbelman*, 2000; *Greeley et al.*, 2000]. On the basis of flow morphology and other considerations, most of these features are interpreted to be the result of effusive basaltic volcanism (e.g., see summary by *Wilson and Head* [1994]). There is also extensive evidence for explosive or pyroclastic activity [e.g., *Mouginis-Mark et al.*, 1982; *Greeley and Crown*, 1990; *Crown and Greeley*, 1993; *Head and Wilson*, 1998; *Plescia*, 2000].

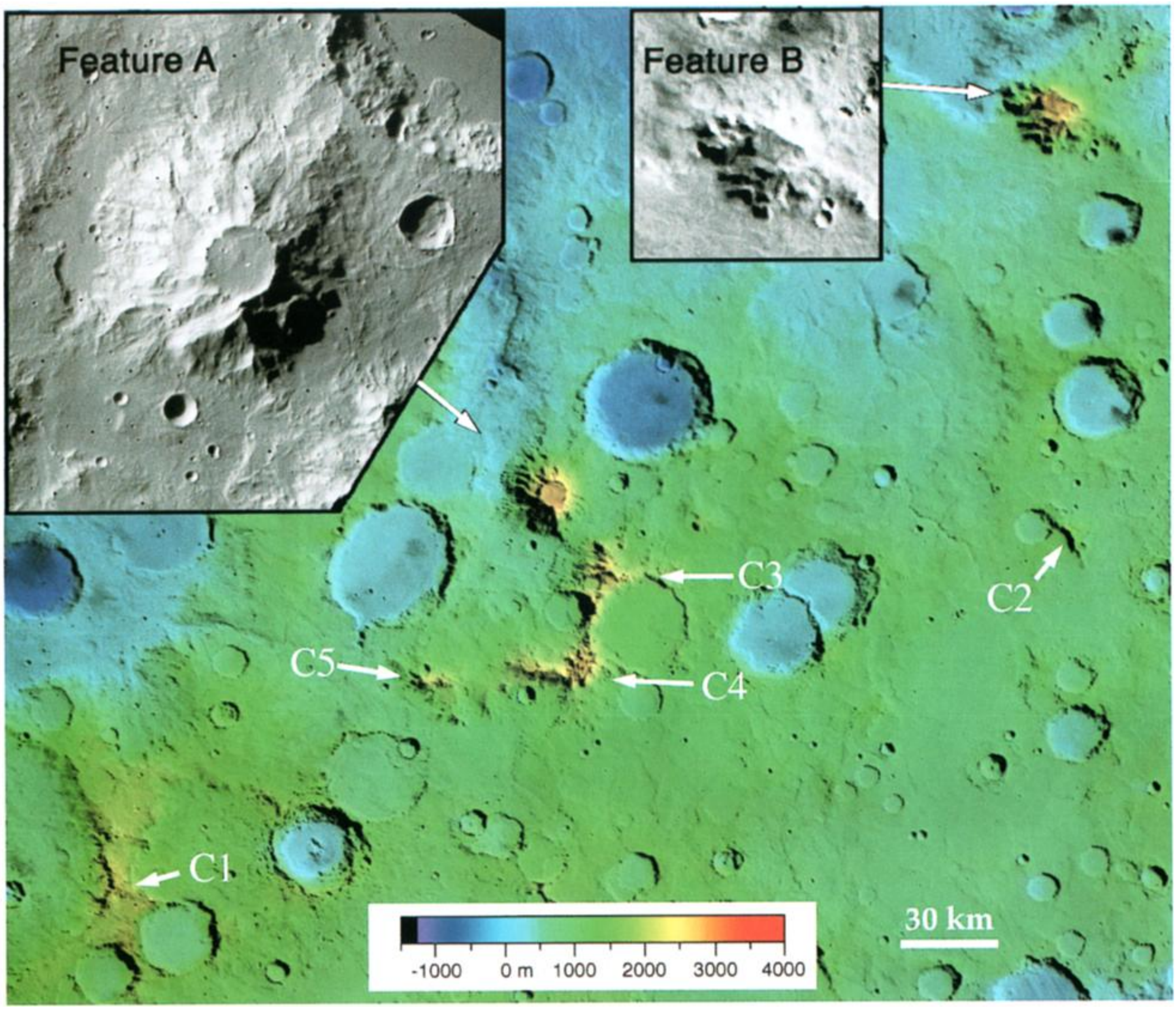

Plate 1. Regional Viking image mosaic overlain on Mars Orbiter Laser Altimeter (MOLA) topography, with superposed images of the features mapped as Nplh in the Aeolis region of Mars. Feature A is Zephyria Tholus. This is Viking image F430S23 of the candidate volcano located at 20°S, 187°W. Image width is 60 km. Note the flat-floored summit crater and the lobate fan deposit in the impact crater to the northeast. Feature B is a Viking image of material mapped as Nplh located at 18°S, 184°W. Note the several domical features with topography similar to Features A and B located to their south (annotated as C1-C5).

Although *Francis and Wood* [1982] argued that few Martian edifices could have a pyroclastic origin on the basis of their low topographic slopes, *Wilson and Head* [1994] demonstrated that because of the difference in atmospheric pressure and gravity on Mars relative to Earth, pyroclastic deposits should be very common on Mars. In addition, volcanic deposits of all kinds are expected to travel farther from the source vent than they would on Earth. This would, in turn, result in volcanic constructs on Mars a factor of 2 broader and a factor of 4 shorter than Earth constructs, calling into question the slope arguments of *Francis and Wood* [1982].

Wilson and Head [1994] demonstrated that volatile nucleation and the resultant disruption of magma can occur in liquids of basaltic composition on Mars because of the low atmospheric pressure. They noted that elevation would have a strong effect on the presence of pyroclastic activity, with greater disruption of magma occurring at higher elevations (when the atmospheric pressure is lower). On the basis of these considerations, *Head and Wilson* [1998] inferred that plinian-style (explosive) eruptions should have been common throughout Martian volcanic history. Increased magmatic volatile content, more silicic magmas, and addition of nonjuvenile volatiles (e.g., groundwater) would all increase the likelihood of explosive pyroclastic activity.

In summary, pyroclastic activity is predicted to be an important process for Mars, even for magmas of basaltic composition. Therefore stratovolcano-like features could be common. However, they are likely to have more subdued topography (lower flank slopes) than Earth stratovolcanoes because of the enhanced dispersal of pyroclastic air fall deposits and enhanced run-out distances typical of Martian pyroclastic flows [e.g., *Wilson and Head*, 1994; *Head and Wilson*, 1998].

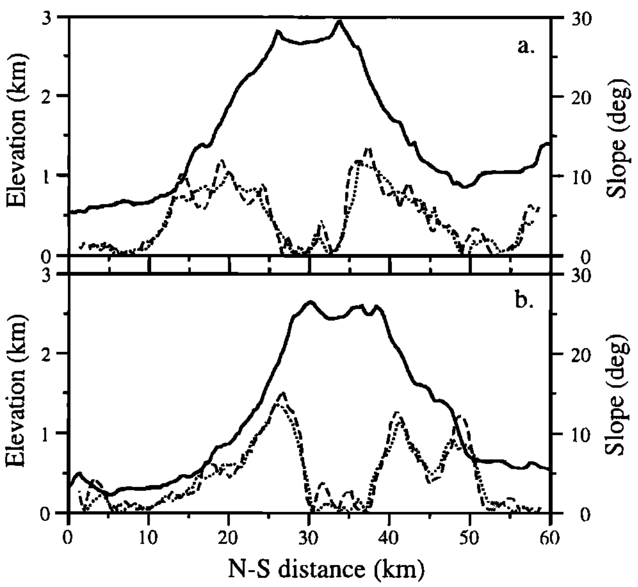

Figure 2. MOLA summit profiles. (a) MOLA profile across Feature A (orbit 12263.2) and point-to-point slopes with 3 km (dashed) and 5 km (dotted) baselines. Vertical exaggeration is 10x. The north flank has slopes as high as 14° near the summit, decreasing approximately linearly with elevation, producing the concave-upward shape typical of a fluvially dissected stratovolcano [*Davidson and de Silva*, 2000]. (b) MOLA pass across Feature B (orbit 12433.1). This also has a concave-upward southern slope and a relatively flat summit, approximating a truncated cone in profile.

4. Topographic Characteristics of Candidate Volcanic Features in the Aeolis Region

The recent acquisition of accurate topography information for Mars using the Mars Orbiter Laser Altimeter (MOLA) [*Smith et al.*, 1998, 1999; *Zuber et al.*, 2000] permits the accurate measurement of the slope and shape of the Aeolis features (Plate 1, Figures 1-3). Here we describe their characteristics, similarities, and differences and assess evidence relevant to a possible volcanic origin.

4.1. Feature A (Zephyria Tholus)

MOLA data show that Feature A (Zephyria Tholus; Plate 1, Feature A) is a truncated cone, characterized by asymmetrical shape and a summit depression (Figures 1a and 2a). The base of the feature averages ~30 km wide and lies at about 500-1000 m elevation, and the present highest point of the rim is ~3000 m, yielding a height of about 2-2.5 km (Figure 1a). Flank slopes approach 14° near the summit and decrease linearly with decreasing elevation (Figures 2a, 3a, and 3b), producing a concave-upward flank shape that is similar to Earth stratovolcanoes that have been fluvially dissected [*Davidson and de Silva*, 2000]. The north flank of the structure appears to have rougher topography (Plate 1, Figures 1a, 2a, 3a, 3b, and 4) because the MOLA track crosses a deeply incised valley. Evidence for dissection by channels is well illustrated on this flank in the perspective view (Figures 3a and 3b); two sinuous channels, each over a kilometer in width, begin near the summit and continue to the base, winding down the slope of the feature and producing a prominent planeze between them. A planeze is a triangular flat-faced facet on the flanks of volcanoes formed by the intersection of two master gullies in the upper reaches of a cone.

At the northeastern base of the structure a lobate flow extends down a crater rim and out onto the crater floor (Plate 1, Figure 3a and 3b). Although this feature appears to be oriented radially to Feature A and could be a volcanic flow emanating from it, the morphological freshness of the lobe and its proximity to a younger impact crater suggest alternatively that it may have been initiated by lobate ejecta emplacement or seismic-energy-induced failure of the crater wall as a result of the impact event.

The other flanks of the edifice also appear to be dissected by channels into planezes and other large angular flank segments. This type of topography could form as a result of differential erosion of flank deposits [e.g., *Davidson and de Silva*, 2000] or, alternatively, as a result of sector collapse of part of the volcano flank when flank deposits became oversteepened [e.g., *van Wyk de Vries et al.*, 2000; *Reid et al.*, 2000]. For the Aeolis features examined in this paper, high-resolution Mars Orbiter Camera (MOC) data are available only for the lower part of the western flank of Feature A (Figure 4d). These images reveal that the edifice is heavily cratered and that the terrain of the lower flanks is characterized by local development of linear and sinuous radial ridges composed of coherent material surrounded by heavily mass-wasted debris deposits. The heavily degraded flank texture could be related to radial volcanic flows and channels (Figure 4f) and is also reminiscent of channel structures on the flanks of Hecates Tholus [*Mouginis-Mark et al.*, 1982].

The truncated summit of the feature consists of a circular depression 8 km wide with a crater rim 200 m higher than the floor (Figures 1a, 2a, 3a, 4a, and 4b). The floor of the summit

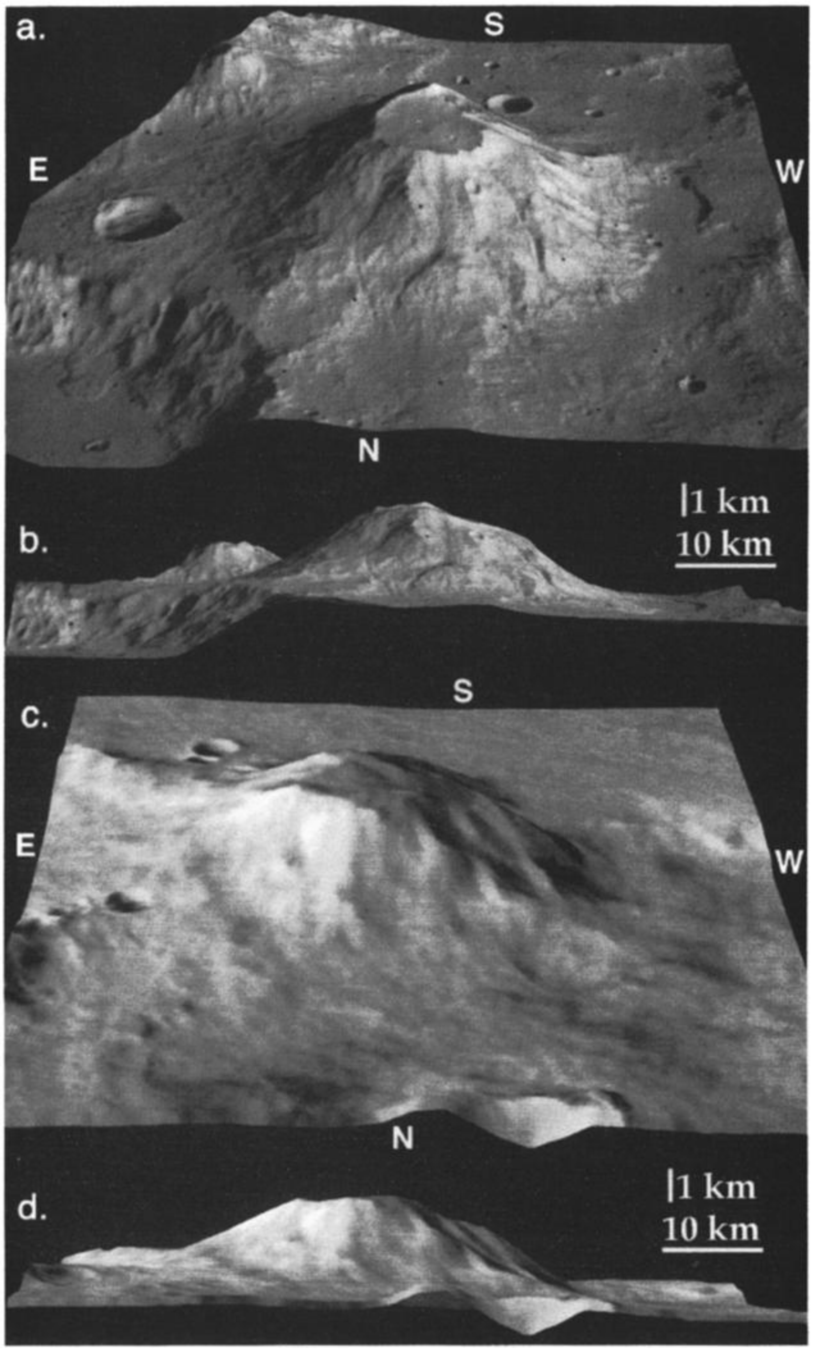

Figure 3. (a and b) Perspective views of Feature A, the highly dissected, Noachian-aged candidate Martian stratovolcano first described by *Greeley and Spudis* [1978]; view is generated by overlaying high-resolution Viking image F430S23 onto a digital elevation model (DEM) using MOLA topography. Vertical exaggeration is ~3x. The crater at the center of the cone is slightly tilted to the northwest. Note the fan deposit in the crater in the northeast. (c and d) Perspective view of Feature B, the topographic high to the northeast of the volcano in Figures 3a and 3b. High-resolution image data are not available for this feature. It is also heavily dissected by valleys and has the same size and slope characteristics as the other feature. Although a summit crater is not obvious from the Viking images, MOLA altimetry reveals a subdued ring-shaped depression in the summit of this feature (Figures 1b and 2b).

crater is relatively smooth (slopes of <1°; Figure 2a) and tilts slightly to the northwest. The circularity of the crater, its distinctly centered summit location, its lack of impact-related features, and the smoothness of its interior all are broadly similar to the characteristics of volcanic calderas on Mars [*Wood*, 1984; *Crumpler et al.*, 1996]. The Feature A summit structure would fall in the Olympus-type caldera category of *Crumpler et al.* [1996], which consists of simple, generally circular or arcuate summit depressions that are often nested. Feature A is most similar to the Elysium Mons subtype, which consists of a single very circular crater in plan form, floored by smooth plains. The size of the Feature A summit crater (~8 km wide and several

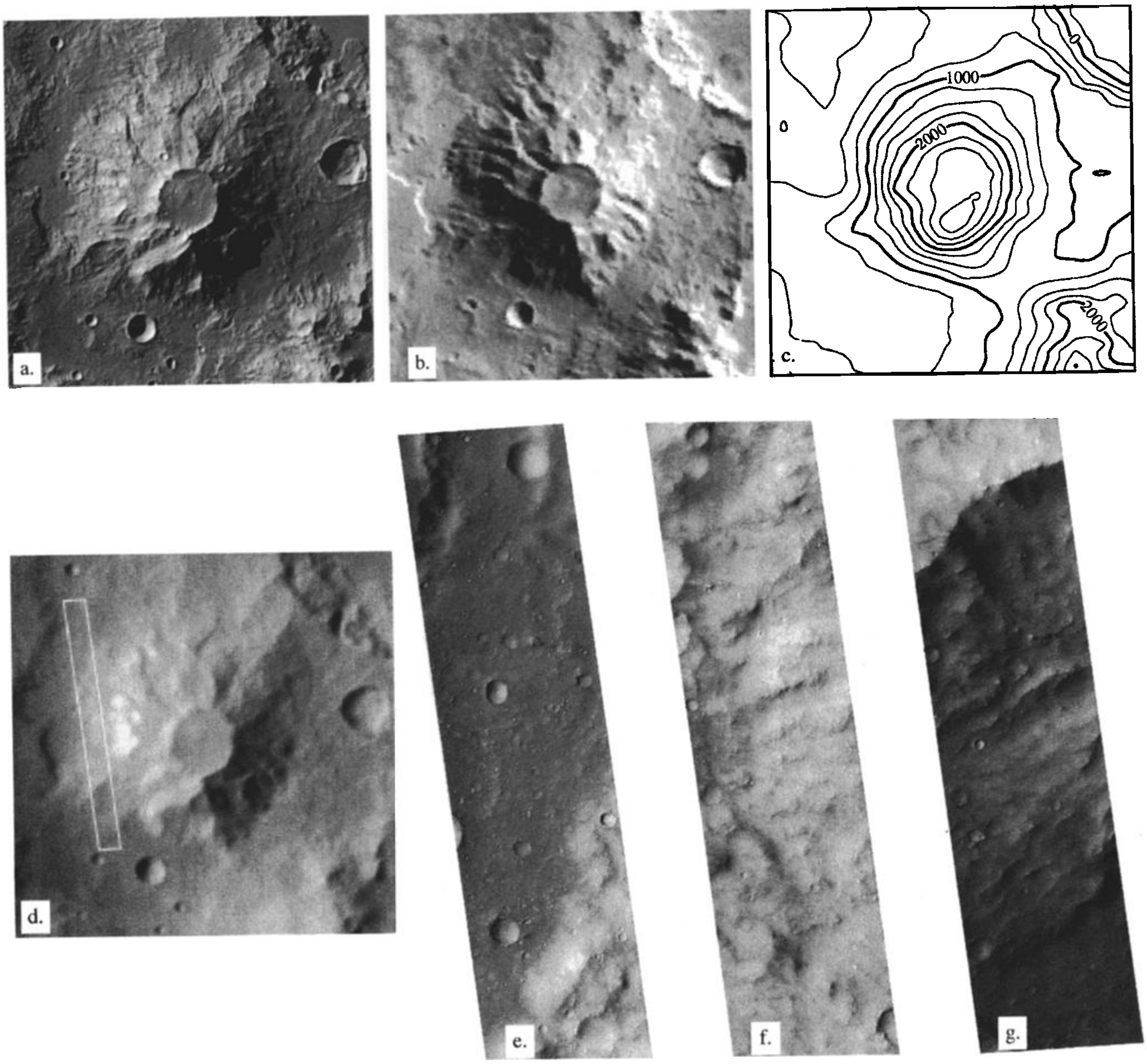

Figure 4. Morphology and topography of Feature A (Zephyria Tholus). (a) Viking image (F430S23) (70 m/pixel). (b) Viking image with different illumination conditions (portion of MDIM MI20S187; ~230 m/pixel). (c) Topographic map derived from MOLA DEM (16 pixels/degree). (d) Viking image with rectangle showing location of MOC image MO3-07208. Portions of Mars Orbiter Camera (MOC) image MO3-07208 (~4 m resolution). Width of image is 2.83 km. (e) Top: smooth plains (upper left) adjacent to the base of the edifice (lower part), which is segmented and heavily cratered. Narrow ridges are arrayed generally radially to the structure and consist of coherent blocky linear scarps surrounded by mass-wasting fragmental material. (f) Middle: ridges and intervening fragmental material are more equidimensional, perhaps related to the large number of subdued craters. The linear scarp at the bottom is the northern margin of the large linear-textured flank deposit seen in the lower image. (g) Bottom: portion of one of the major valleys that extend radially from the summit area down the flanks; narrow linear to sinuous ridges are arrayed generally parallel to the strike of the valley and are surrounded by mass-wasted finer debris. This portion of the deposit is heavily cratered, with a narrow channel (about 200-300 m wide) visible in the upper middle part of the image. At the base of the image, adjacent surrounding smooth plains are observed. (h) Annotated MOLA profile along MOC image showing local topography over the flank of the feature.

hundred meters deep) is at the lower end of the range of caldera diameters and depths for Mars [*Crumpler et al.*, 1996, Figures 23 and 24], consistent with the small diameter of the edifice.

Comparison of the morphometry of Feature A and data for 216 terrestrial stratovolcanoes [*Pike*, 1978, Table 2] shows that the height and summit crater width/depth ratios are in the range of terrestrial values and that the edifice diameter is toward the higher end of the terrestrial values. However, pyroclastic air falls and flows should be more widely dispersed on Mars [*Wilson and Head*, 1994], and thus edifices built with pyroclas-

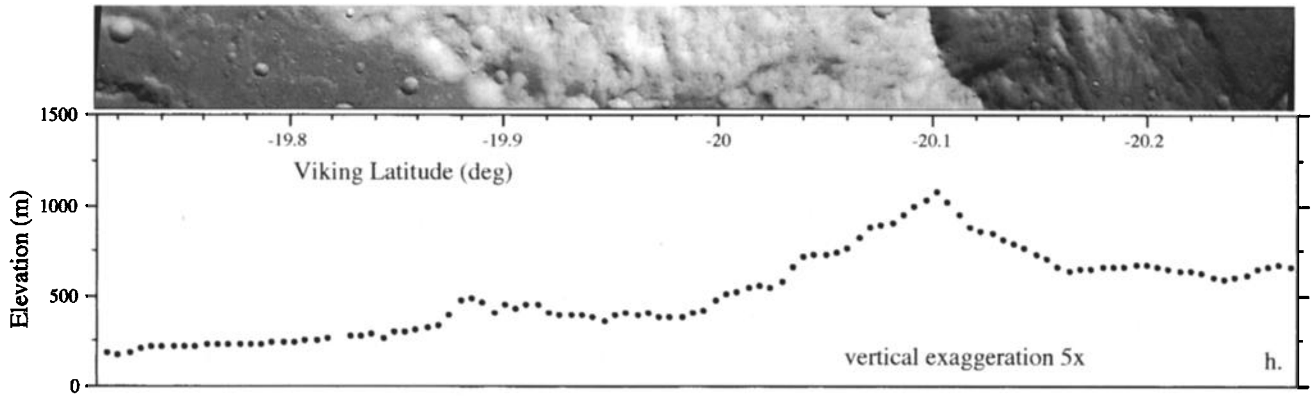

Figure 4. (continued)

tic eruption contributions are predicted to be broader than similar structures on Earth, potentially accounting for the diameter of Feature A relative to terrestrial edifices.

Among the several plausible origins for high topography in ancient terrain are (1) multiple overlapping impact crater rims consisting of topography due to structural uplift and emplacement of ejecta preferentially on the rims; (2) tectonic scarps caused by faulting and production of differential topography; (3) volcanic construction, caused by edifice-building processes (extrusive and explosive eruption products around a vent), and (4) preferential erosion, including exhumation of preexisting topographic features, or simple production of inselbergs due to the regional stripping of units.

On the basis of the symmetry, truncated cone shape, presence of a summit crater that was apparently resurfaced by smooth plains, and the lack of adjacent impact craters that might have produced high topography through multiple overlapping impact crater rims, we find that MOLA data support earlier interpretations [e.g., *Greeley and Spudis*, 1978; *Hodges and Moore*, 1994] that Feature A is an edifice of volcanic origin. We find no compelling evidence for the previous presence and subsequent stripping of a layer on the order of 2 km in thickness to produce this feature, nor do we find evidence for regional faulting that might have produced this feature.

Adopting the interpretation that the structure is a volcano with a summit caldera, we estimated a possible original precaldera size of the volcano by fitting parabolic curves to the topography of its flanks (Figure 5). The curves meet at a maximum peak elevation of ~3.9 km, giving the volcano a possible overall original height of ~3 km, comparable to the height of terrestrial stratovolcanoes [*Pike*, 1978].

4.2. Feature B

To the northeast of Feature A (Plate 1) is a second dissected domical feature (Feature B; 18°S, 184°W) that lacks an obvious summit crater. Its base is approximately the same size (~30 km) as that of Feature A, and the two mountains have similar elevation ranges (Feature B is ~2 km in height) (compare Feature A in Figures 1a, 2a, 3a, and 3b to Feature B in Figures 1b, 2b, 3c, and 3d). Its slope characteristics and its cross-sectional profile are strikingly similar to those of Feature A (compare Figures 1 and 2). Although no summit crater is obvious from the low-resolution Viking images, the MOLA profile reveals a flat but complex summit structure consisting of a small summit depression containing a central hill (Figure 1b). Although broadly similar to features such as Mount St. Helens, with its summit crater and younger dome, the Viking resolution is not sufficient to assess this possibility, and no MOC images of this feature are currently available. The flanks of the feature are characterized by numerous triangular-shaped blocks with one tip of the triangle pointing up slope. Although the detailed morphology and relation to possible flank channels are not completely clear owing to relatively low image resolution, the similarity to features on the flanks of Feature A (Plate 1; Figures 3 and 4) suggests the possibility that these features are planezes or sector collapse remnants.

Viking images (Plate 1, Feature B) show that the northeastern flank of this feature appears broadly linear, and the feature itself, in contrast to Feature A, is elongated, trending in a general NW-SE direction. If this linearity represents the presence of a fault scarp, evidence for it is not prominent, nor is there additional topography along the strike approaching this altitude that might be related to a fault scarp. Another possible

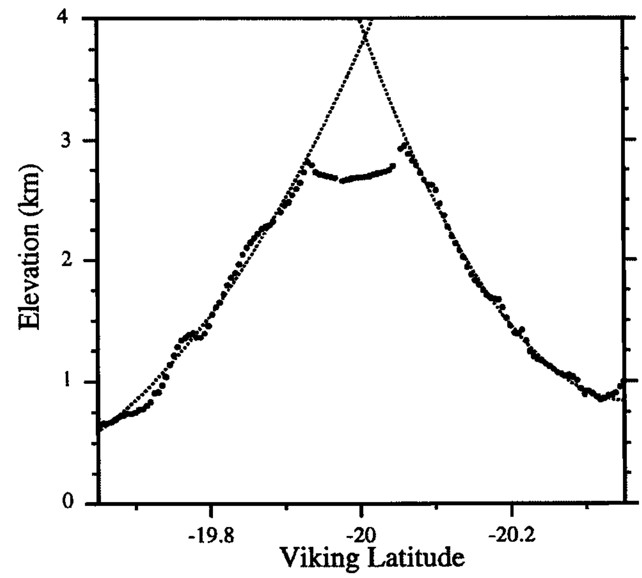

Figure 5. MOLA profile across Feature A, the candidate stratovolcano (orbit 12263.2). Parabolic curves were fit to the MOLA laser shot points by a least squares method to reconstruct its possible original elevation. Vertical exaggeration is 10x. The minimum reconstructed relative height of the volcano is ~3 km but could be higher depending on the degree to which the flank elevation has been lowered by fluvial dissection and mass wasting.

origin could be a degraded impact crater rim. Broad depressions exist to the northwest and east, which may represent topography associated with heavily degraded craters, but the topography is very subdued and no other evidence is seen of high topography that might be due to coalescing rim deposits.

The similarity of this feature to Feature A in terms of approximate size, height, and flank slopes, its topographic distinctiveness from the surrounding plains, and its lack of close correlation with rugged multiple overlapping impact crater rims and prominent fault scarps all support a volcanic origin. Feature B differs from A in its more irregular and elongated nature, the lack of a distinctive summit crater (although the summit is relatively flat), and the more prominent planezes on its flanks.

4.3. Other Features

A number of other topographic highs appear in the region shown in Plate 1 (labeled C1-C5); these are similar to Features A and B in that they are about 20-50 km in diameter and stand distinctly (~750-1250 m) higher than the surrounding plains. Could these be volcanic edifices or more degraded versions of Features A and B? The broad high ~180 km southwest of Feature A (Plate 1, C1, lower left) is topographically diffuse, with low slopes and a close association with a large impact crater ~80 km in diameter just to the west. This topography appears to be best explained by the additive ejecta and structural uplift of this crater, a very ancient one just to the east, and two younger craters (about 20 and 25 km diameter) just to the south. A second smaller occurrence is seen ~150 km east of Feature A (Plate 1, labeled C2 in eastern part of the image). This feature is small and irregular in shape (about 10 by 20 km), is low (~500 m high), and is not obviously associated with major impact craters. Insufficient data are available to assess its origin.

A third occurrence is observed just south of Feature A (Plate 1; labeled C3-C5; central part of image). In this case, there are several coalescing positive topographic features forming an irregularly shaped structure. Part of the distinctive topography is due to the presence and rim of a relatively fresh 30 km diameter crater that has been superposed on what appears to be preexisting high topography. The characteristics of the high topography are similar in many ways to those of the flanks of Features A and B; there are channel-like features on the flanks, and candidates for topographic blocks resembling planezes and possible sector collapse (Plate 1; Figures 2-4). Although subsequent impact craters have considerably modified the original deposits, the remaining high topography stands prominently above the surrounding plains at approximately the same level as the nearby Feature A. These terrain characteristics, and their proximity to Feature A, lead us to suggest that these features could be remnants of volcanic edifices perhaps originally comparable to Feature A but highly modified by subsequent impacts. Present data are insufficient to address this issue; additional data acquisition involving high-resolution mineralogical and imaging information is required to clarify this important issue.

5. Discussion and Conclusions

On the basis of the new MOLA data for individual features and the topography of the Aeolis region as a whole, we conclude that Feature A (Zephyria Tholus) is of volcanic origin and that Feature B is also very likely to be of volcanic origin. Some of the other diffuse high topography in Aeolis is more likely to be related to coalesced crater rim deposits, but the unusual occurrence just south of Feature A may be ancient additional volcanic constructs that have been heavily modified by subsequent impact cratering.

The topographic features illustrated in Figure 2 have a size similar to large Earth stratovolcanoes, but Earth stratovolcanoes have much steeper flank slopes [*Walker*, 2000] than do Martian features. This morphology, however, is similar to that predicted for pyroclastic eruptions under Martian conditions [*Wilson and Head*, 1994]. We therefore conclude that Features A and B observed in the Aeolis region of Mars are likely candidates for a stratovolcanic origin, with the reservation that their presently degraded state (Figure 4) prevents the observation and documentation of features associated with pyroclastic deposits. Although the fragmental materials and evidence of mass wasting seen at very high resolution on the flanks of Feature A in MOC images (Figure 4) could be pyroclastic deposits, the age and degraded state of the edifice precludes confident interpretation of the origin of these deposits.

The apparent ancient age (Noachian) [*Scott and Tanaka*, 1986; *Greeley and Guest*, 1987] of these features, if correct, provides further evidence that volcanic activity was an important contribution to the formation and evolution of the Noachian highlands. The relatively fresh appearance of Feature A could mean that it is of slightly younger Hesperian age, coincident with other Hesperian-aged volcanic and fluvial activity in the region [e.g., *Nelson*, 2001a, 2001b]. In any case, the criteria outlined here for the origin of isolated knobs and topographic highs can be used to help distinguish the range of origins and the possibility of volcanic edifices in ancient deposits elsewhere on Mars. These criteria include (1) size, (2) slope characteristics, (3) evidence of planezes and other dissection processes common to, but not necessarily uniquely associated with, pyroclastically built volcanoes, and (4) the inability to explain by other hypotheses such as coalescing impact crater rims, exhumation, etc. Although there is evidence for pyroclastic activity throughout the history of Mars, the style of volcanism in earlier history (Noachian-Hesperian) clearly included more abundant examples of pyroclastic activity than later examples [e.g., *Greeley and Spudis*, 1981; *Greeley and Crown*, 1990; *Crown and Greeley*, 1993]. The morphology and morphometry of Feature A are consistent with an origin from deposits of mixed pyroclastic and effusive eruptions. Although the features analyzed in this study are broadly aligned, there is no evidence that they are related to subduction zones proposed by *Sleep* [1994] for this time interval.

Acknowledgments. We thank Stephen Pratt for preparation of data for use in these analyses and for discussion of science results and Peter Neivert for help in preparation of the figures. Gil Ghatan and Brian Nixon helped in the preparation of the MOC images and in the discussion of the results. Jim Zimbelman provided an extensive and helpful review. This research was supported by NASA PG & G Grant NAG5-4723 and MDAP "Martian Volcanic Edifice Characterization" grant NAG5-9780 to J.W.H., which are gratefully acknowledged.

References

Bates, R., and J Jackson, *Dictionary of Geological Terms*, Am. Geol. Inst., Washington, D. C, 1984.

Cas, R, and J Wright, *Volcanic Successions*, Allen and Unwin, Concord, Mass., 1987.

Crown, D. A., and R. Greeley, Volcanic geology of the Hadriaca Patera and the Eastern Hellas region of Mars, *J. Geophys. Res.*, *98*, 3431-3451, 1993.

Crumpler, L. S., J. W Head, and J C Aubele, Calderas on Mars. Characteristics, structure, and associated flank deformation, in *Volcano Instability on the Earth and Other Planets*, edited by W J. McGuire et al., *Geol. Soc. Spec. Publ., 110*, 307-348, 1996

Davidson, J., and S. de Silva, Composite volcanoes, in *Encyclopedia of Volcanoes*, edited by H Sigurdsson, pp. 663-681, Academic, San Diego, Calif., 2000

Francis, P. W., and C. A Wood, Absence of silicic volcanism on Mars: Implications for crustal composition and volatile abundance, *J. Geophys. Res., 87*, 9881-9889, 1982.

Greeley, R., and D. A Crown, Volcanic geology of the Tyrrhena Patera region of Mars, *J. Geophys. Res., 95*, 7133-7149, 1990

Greeley, R., and J E. Guest, Geological map of the eastern equatorial region of Mars, *U S Geol Surv. Misc Invest. Map, I-1802B*, 1987.

Greeley, R., and P. D. Spudis, Volcanism in the cratered terrain hemisphere of Mars, *Geophys Res Lett., 5*, 453-455, 1978

Greeley, R., and P. D. Spudis, Volcanism on Mars, *Rev. Geophys, 19*, 13-41, 1981.

Greeley, R., N. T Bridges, D. A. Crown, L. Crumpler, S A. Fagents, P. J. Mouginis-Mark, and J R. Zimbelman, Volcanism on the red planet, Mars, in *Environmental Effects on Volcanic Eruptions*, edited by J. R Zimbelman and T K P. Gregg, pp. 113-142, Kluwer Acad, Norwell, Mass., 2000.

Gregg, D. R., The geology of Tongariro Subdivision, *N. Z Geol. Surv. Bull., 40*, 152 pp, 1960.

Head, J. W, and L. Wilson, Tharsis Montes as composite volcanoes?: 1. The role of explosive volcanism in edifice construction and implications for the volatile contents of edifice-forming magmas, *Lunar Planet. Sci.* [CD-ROM], *XXIX*, abstract 1127, 1998.

Hodges, C. A., and H. Moore, Atlas of volcanic landforms on Mars, *U.S. Geol Surv. Prof Pap. 1534*, 194 pp, 1994.

Mouginis-Mark, P. J, L. Wilson, and J W. Head, Explosive volcanism of Hecates Tholus, Mars: Investigation of eruption conditions, *J. Geophys. Res, 87*, 9890-9904, 1982.

Nelson, D. M., J. D. Farmer, R. Greeley, R. O Kuzmin, and H P. Klein, Durius Valles outflow basin, Mars: Proposed site for MER-A, *LPI Contrib. 1079*, pp. 55-56, Lunar and Planet. Inst., Houston, Tex., 2001a.

Nelson, D. M., J. D. Farmer, and R. Greeley, Hydrologic history of south Elysium basin-north Terra Cimmeria area, Mars, *Lunar Planet. Sci.* [CD-ROM], *XXXII*, abstract 2069, 2001b.

Pike, R J., Volcanoes on the inner planets: Some preliminary comparisons of gross topography, *Proc. Lunar Planet Sci. Conf. 9th*, 3239-3273, 1978

Plescia, J. B., Geology of the Uranius Group volcanic constructs: Uranius Patera, Ceraunius Tholus, and Uranius Tholus, *Icarus, 143*, 376-396, 2000

Reid, E., S. B. Christian, and D L Brien, Gravitational stability of three-dimensional stratovolcano edifices, *J. Geophys Res., 105*, 6043-6056, 2000

Scott, D. H, and K L. Tanaka, Geological map of the western equatorial region of Mars, *U S. Geol. Surv Misc Invest. Map, I-1802A*, 1986.

Sleep, N. H., Martian plate tectonics, *J. Geophys. Res, 99*, 5639-5655, 1994

Smith, D E., et al, Topography of the northern hemisphere of Mars from the Mars Orbiter Laser Altimeter (MOLA), *Science, 279*, 1686-1692, 1998.

Smith, D E., et al, The global topography of Mars and implications for surface evolution, *Science, 284*, 1495-1503, 1999.

van Wyk de Vries, B, N Kerle, and D. Petley, Sector collapse forming at Casita volcano, Nicaragua, *Geology, 28*, 167-170, 2000.

Walker, G. P. L., Basaltic volcanoes and volcanic systems, in *Encyclopedia of Volcanoes*, edited by H Sigurdsson, pp. 283-289, Academic, San Diego, Calif., 2000.

Wilson, L., and J. W. Head, Mars: Review and analysis of volcanic eruption theory and relationships to observed landforms, *Rev. Geophys., 32*, 221-263, 1994.

Wood, C. A., Calderas: A planetary perspective, *J. Geophys. Res., 89*, 8391-8406, 1984.

Zimbelman, J R., Volcanism on Mars. in *Encyclopedia of Volcanoes*, edited by H. Sigurdsson, pp. 771-783, Academic, San Diego, Calif., 2000.

Zuber, M., et al., Internal structure and early thermal evolution of Mars from Mars Global Surveyor topography and gravity, *Science, 287*, 1788-1793, 2000

J W. Head and E. M. Stewart, Department of Geological Sciences, Brown University, Box 1846, Providence, RI 02912. (James_Head_III@brown.edu)

(Received July 18, 2000, revised February 26, 2001; accepted March 9, 2001)